ACS APPLIED MATERIALS & INTERFACES

Research Article

www.acsami.org

DMSO–Li_2O_2 Interface in the Rechargeable Li–O_2 Battery Cathode: Theoretical and Experimental Perspectives on Stability

Marshall A. Schroeder,[†] Nitin Kumar,[§,∥] Alexander J. Pearse,[†] Chanyuan Liu,[†] Sang Bok Lee,[‡] Gary W. Rubloff,[†] Kevin Leung,[§] and Malachi Noked*[,‡]

[†]Department of Materials Science and Engineering, University of Maryland, College Park, Maryland 20742, United States

[§]Sandia National Laboratories, Albuquerque, New Mexico 87185, United States

[∥]Department of Mechanical Engineering, University of Michigan, Ann Arbor, Michigan 48109, United States

[‡]Department of Chemistry and Biochemistry, University of Maryland, College Park, Maryland 20742, United States

Supporting Information

ABSTRACT: One of the greatest obstacles for the realization of the nonaqueous Li–O_2 battery is finding a solvent that is chemically and electrochemically stable under cell operating conditions. Dimethyl sulfoxide (DMSO) is an attractive candidate for rechargeable Li–O_2 battery studies; however, there is still significant controversy regarding its stability on the Li–O_2 cathode surface. We performed multiple experiments (in situ XPS, FTIR, Raman, and XRD) which assess the stability of the DMSO–Li_2O_2 interface and report perspectives on previously published studies. Our electrochemical experiments show long-term stable cycling of a DMSO-based operating Li–O_2 cell with a platinum@carbon nanotube core–shell cathode fabricated via atomic layer deposition, specifically with >45 cycles of 40 h of discharge per cycle. This work is complemented by density functional theory calculations of DMSO degradation pathways on Li_2O_2. Both experimental and theoretical evidence strongly suggests that DMSO is chemically and electrochemically stable on the surface of Li_2O_2 under the reported operating conditions.

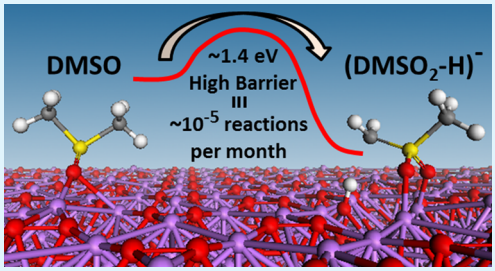

KEYWORDS: *dimethyl sulfoxide (DMSO), lithium oxygen battery, density functional theory (DFT), lithium peroxide (Li_2O_2), atomic layer deposition (ALD)*

INTRODUCTION

Realization of the theoretical capacity of rechargeable, aprotic Li–O_2 batteries has the potential to transform electrochemical energy storage, reaching gravimetric energy densities 3–5 times higher than current secondary Li-ion chemistries.[1,2] This system involves the three phase reaction of Li^+ and O_2 on a conductive porous scaffold immersed in an aprotic environment.[3] During discharge, the oxygen reduction reaction (ORR) on the positive electrode forms insoluble Li_2O_2 as Li^+ from the organic electrolyte reacts with reduced oxygen species at a theoretical potential of 2.96 V vs Li/Li^+.[3] This reaction challenges the chemical stability of the electrolyte and cathode scaffold with highly oxidizing intermediates and products (O_2^-, O_2^{2-}, and Li_2O_2). During charge, the lithium peroxide should theoretically be dissociated via the oxygen evolution reaction (OER) at potentials below 3.2 V vs Li/Li^+.[2−6] This reverse reaction has been shown to require high overpotentials, leading to possible anodic or chemical oxidation of the electrolyte and cathode by the evolved species and dissolved O_2 at high potentials. The degradation of cell components at very early stages of cell life complicates the realization of this system, making it difficult to separate side reactions from the actual ORR\OER.[1,3−6] Thus, finding a sufficiently stable electrolyte is considered the greatest challenge for realizing the Li–O_2 rechargeable system both fundamentally and practically.[7−13]

Both experimental and theoretical works surveying various solvent candidates for Li–O_2 electrolytes have struggled to find an appropriate solvent for the study and development of rechargeable Li–O_2 batteries. Carbonate-based electrolytes used in early Li–O_2 works were later found to be unstable against ORR reaction intermediates and form Li-carbonate species instead of the lithium peroxides or oxides expected for healthy ORR.[3,10,13,14] Polyether solvents were reported to degrade in the presence of O_2, Li^+, and reduced oxygen either by auto-oxidation[15] or electrooxidation.[8,12,15] One of the other widely used solvents for Li–O_2 batteries is dimethyl sulfoxide (DMSO); however, due to multiple contradicting reports on its chemical stability on the surface of Li–O_2 cathode, there is a strong need to carefully assess its stability before continuing to use it in Li–O_2 R&D.

DMSO in Aprotic Li–O_2 Batteries. Extensive research has focused on the stability of DMSO as a medium for oxygen electrochemistry. Laoire et al. examined DMSO for Li–O_2 batteries, suggesting it as a promising solvent for stabilization of reduced oxygen species during ORR.[10] Various groups then demonstrated cells operating with DMSO-based electrolytes,

Received: March 4, 2015
Accepted: May 6, 2015
Published: May 6, 2015

DOI: 10.1021/acsami.5b01969
ACS Appl. Mater. Interfaces 2015, 7, 11402−11411

leading to improvements in cycle life[10] and the stability of the cathode;[16] however, recent publications suggested a mechanism for chemical or anodic oxidation of DMSO in Li−O_2 operating cells under certain conditions that can cause detectable solvent decomposition.[17,18] Furthermore, two separate reports suggested either spontaneous chemical degradation of Li_2O_2 into carbonate when in contact with DMSO (monitored by XPS)[19] or complete decomposition of Li_2O_2 to LiOH conjugated with extensive oxidation of DMSO to dimethyl sulfone ($DMSO_2$ detected by FTIR),[20] and concluded that DMSO is not an appropriate solvent for studying Li−O_2 batteries with long discharge durations due to its chemical instability on the surface of Li_2O_2, bringing into question the relevancy of earlier reports involving more practical systems. We will further address the conditions presented in these two reports and present contradicting results under robust conditions for monitoring Li_2O_2 degradation or DMSO oxidation.

Indeed, concerns regarding DMSO stability in the presence of superoxide ions goes back to reports published by Sawyer and co-workers,[21,22] suggesting possible oxidation of DMSO to $DMSO_2$ in a solution containing tetraethylammonium perchlorate (TEAP) salt. However, this oxidation was not suggested to involve hydrogen abstraction from DMSO or a direct nucleophilic attack by O_2^- on the sulfur atom of the S═O bond but rather involved an initial hydrogen abstraction from the alkylammonium ion and was tested in relatively high water content (>500 ppm of H_2O), which can also serve as a possible source of protons. The nucleophilic attack suggested by Sawyer and co-workers therefore occurs by hydroperoxy ions and not O_2^-. A summary of the suggested mechanisms is presented in Scheme S1. Anodic oxidation of DMSO to $DMSO_2$ was also found possible by Krtil et al.[23] using Li salts in DMSO but with an extremely high concentration of water (~0.04 M) compared to properly dehydrated Li−O_2 systems. This work was recently validated in a more controlled environment by Calvo and co-workers,[18] reporting the appearance of $DMSO_2$ at potentials above 4.2 Vs Li\Li^+ via processes also hypothesized to be involved in consumption of trace water from the electrolyte.

All of the above work used FTIR for characterization, and the peak of the symmetric SO_2 stretch ($\nu_S SO_2$) at 1142 cm^{-1} was considered a marker for the presence of $DMSO_2$. The limit of detection (LOD) of the FTIR system for the presence of $DMSO_2$ in the solvent has not been reported in these works, making it difficult to quantitatively evaluate the extent of the reported oxidation. This calibration is critical to determine if the observed peaks indicate continuous oxidation of the solvent or only a minor parasitic reaction that may stop (i.e., after ppm level H_2O is fully consumed), having no significant effect on cell performance and cyclability. Furthermore, the observed peaks in the 1140−1145 cm^{-1} range are not exclusively indicative of $DMSO_2$, as shown in recent works done with in-operando Raman spectroscopy[24] and surface enhanced Raman[9] (SERS), which attribute the peak at ~1140 cm^{-1} to the formation of LiO_2 on the surface of the cathode rather than the oxidation of DMSO to $DMSO_2$. Indeed, these Raman experiments did not suggest DMSO oxidation; however, the exposure time of DMSO to Li_2O_2 and superoxide ions in these reports was relatively short.[20]

In order to deconvolute the question of DMSO stability on the Li_2O_2 surface in operating a Li−O_2 battery, we demonstrate a computational exploration of the chemical stability of the Li_2O_2/DMSO interface using density functional theory (DFT) and propose a novel reaction pathway supported by calculated activation energies. Furthermore, we carefully address the previously reported conditions for chemical decomposition of DMSO by using a specialized UHV integrated system for sample preparation and transfer to XPS without exposure to air or moisture for analysis of Li_2O_2 aged in DMSO. FTIR and Raman spectra were collected for each chemical species in our report and previous reports, in addition to the limit of detection (LOD) of our FTIR and Raman systems for the detection of $DMSO_2$. We also investigate DMSO stability against oxidation during ORR or anodic oxidation under operating Li−O_2 battery conditions. The Li_2O_2 aged in DMSO showed no definitive chemical changes with time, and $DMSO_2$ could not be detected with FTIR, even after 7 months. Furthermore, mesoporous core−shell Pt@CNT cathodes synthesized via atomic layer deposition enabled us to demonstrate the stability of DMSO during cycling for over 4 months of cell operation, with a round-trip cycle duration of 80 h and with more than 45 cycles before disassembling the cell for spectroscopic characterization.

We find that DMSO is highly stable on the surface of Li_2O_2, both theoretically and experimentally. We also clearly demonstrate that oxidation reported to occur in the presence of KO_2 and detected by stretching spectroscopies can be attributed to the presence of KO_2.

EXPERIMENTAL STUDIES

$DMSO_2$ as an Indicator of DMSO Oxidation. Previous reports used FTIR for detection of SO_2 stretching, suggesting this stretching indicates the oxidation of DMSO. It has become accepted to use KO_2 as a source for superoxide in DMSO and to chemically monitor the degree of oxidation of the solvent, as indicated by the appearance of stretching peak at 1142 cm^{-1} using Raman or FTIR. However, as presented in Figure S1, the Raman spectrum of pristine KO_2 shows a strong peak at 1142 cm^{-1} (which can be attributed to O═O stretching), strongly implying that KO_2 is not a suitable source of superoxide in a solution where $DMSO_2$ is to be measured at any concentration. This observation agrees well with FTIR reports of pristine KO_2, and the literature value of $\upsilon_{O=O}$ = 1145 cm^{-1}.[9,24,25] It seems like the only appropriate way to use KO_2 in order to test oxidation of DMSO to $DMSO_2$ by stretching spectroscopy is to use $K^{18}O_2$ in which the $\upsilon_{O=O}$ is shifted to 1118 cm^{-1}.[25] The decomposition of KO_2 under the laser also manifested additional peaks suggesting that the O−H peak previously reported by others as $LiOH_2O$ could be attributed to decomposition of KO_2 to KOH and not necessarily to Li_2O_2 decomposition to LiOH (see Figure S1). We first calibrated the FTIR to determine the limit of detection (LOD) for $DMSO_2$ in DMSO. Figure S2 shows that the SO_2 peak will manifest itself even at concentrations below 500 ppm, implying that FTIR will sense the presence of SO_2 at very low concentrations (LOD < 7 mM). Figure S3 shows the same calibration process performed with Raman, showing that the LOD of Raman is higher at about 1% (140 mM), suggesting that Raman can confirm or rule out extensive oxidation of DMSO to $DMSO_2$.

To test the possible oxidation of DMSO in an operating Li−O_2 cell (in the presence of O_2 reduced oxygen species), we discharged a MWCNT cathode to 3000 $mAhg^{-1}$ at 100 mAg^{-1}, let it rest for 14 days inside the glovebox, and opened the cell inside the glovebox to collect a sample of the electrolyte for Raman testing. As presented in Figure 1, there is no signal for the symmetric SO_2 stretch (1142 cm^{-1}) in the electrolyte despite an expected molar concentration >2% according to degradation suggested in a previous report[20] (please see the SI

DOI: 10.1021/acsami.5b01969
ACS Appl. Mater. Interfaces 2015, 7, 11402−11411

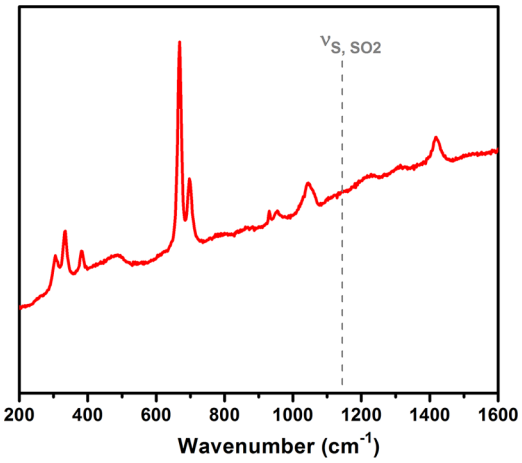

Figure 1. Raman spectrum of electrolyte after 14 days of rest within a discharged cell. No signal at 1142 cm^{-1} suggests oxidation of DMSO is below detection limits or not present at all.

for more information). We tested the solubility of $DMSO_2$ in DMSO to confirm that this proposed decomposition product should be detected in solution, if present, and found a saturation limit of 20 mol % of $DMSO_2$ in DMSO (see the SI).

Long-Term Stability of DMSO Against Oxidation in an Operational Li−O_2 Cell. In a practical Li−O_2 cell the stability needs to be tested very long-term, as pointed out by Shao-Horn and co-workers.[20] However, the majority of the cathodes used in Li−O_2 reports are either carbon cathodes which demonstrate high gravimetric capacity but limited cycle life[26] (~15 or fewer high capacity cycles due to chemical and electrochemical instability of the carbon) or porous cathodes made of gold or TiC that undergo discharge processes of relatively short times[16,27] (less than 2 h for the reports on the porous gold electrodes by Bruce et al.). Additionally, the anodic instability of DMSO at potential higher than 4−4.3 V[17,18] vs Li in the presence of O_2 and H_2O (even trace amounts)[18] was reported to manifest $DMSO_2$ in the electrolyte upon cycling, making it difficult to isolate whether detected oxidation took place on the Li_2O_2/DMSO interface upon prolonged exposure or by anodic oxidation of DMSO at high potentials. In order to fabricate the Li−O_2 cathode that will enable both long discharge and extended cycle life, and will enable the testing of DMSO stability in the presence of O_2 and reduced oxygen species in a Li−O_2 cell, we synthesized the core−shell Pt@CNT cathode by atomic layer deposition of Pt on self-standing CNT. The structure of the Pt@CNT cathode is presented in TEM and SEM images in Figure 2.

The details of the synthesis and more comprehensive description of the electrochemical performances are beyond the scope of this paper and will be discussed in more detail elsewhere, but this cathode enabled us to test the long-term stability of DMSO, toward oxidation, in operating a Li−O_2 cell. The cyclic voltammetry (CV) response of the bare sponge and the Pt decorated MWCNT cathodes are presented in Figure S4 with a relevant discussion. The Pt shell enabled pronounced catalytic activity for OER, hence a significant amount of the discharge capacity could be recovered upon charge at voltages below the reported value for anodic oxidation of DMSO.[18,23] Long-term cycling stability of this system was tested via galvanostatic cycling with currents of 50 mAg^{-1}_{carbon} with fixed discharge capacities of 2,000 $mAhg^{-1}_{carbon}$. This translates to a 40 h discharge followed by a 4 V voltage-limited charge step for more than 45 cycles. To our knowledge, this is one of the longest individual cycle durations reported in a study of a rechargeable Li−O_2 cathode. After this duration of cycling the cell was purged with Ar and disassembled inside the glovebox, and a sample of electrolyte was taken for Raman and tested for the presence of $DMSO_2$. If DMSO oxidation had taken place on the Li_2O_2 surface as previously suggested, the expected concentration of $DMSO_2$ should exceed 35 mol % after 4 months of operation (SI). Yet, as presented in Figure 3, no $DMSO_2$ was detected even after these extremely long cycle times, strongly suggesting that the degree of oxidation of DMSO was below 1 mol % and had a negligible effect on battery cycling performance. For a comparison, a Raman spectrum of 20 mol % $DMSO_2$ in DMSO is also presented. In addition to the standard marker (1142 cm^{-1}), three other peaks which are characteristic of $DMSO_2$ were also observed (465, 495, and 763 cm^{-1}) in this comparison but are absent from the Pt@CNT electrolyte.[28]

The lowest potential for ORR in this cell was above 2.65 V, higher than the potential reported to decompose DMSO on a microporous carbon cathode,[17] and the Pt@CNT is hypothesized to possess a significantly lower concentration of an acidic functional group as compared to microporous carbon; hence, it is less likely to induce formation of the hydroperoxy ion that can oxidize DMSO through nucleophilic attack on sulfur in DMSO.[17,18,21]

Li_2O_2 Decomposition. We have also examined the surface chemistry of Li_2O_2 in contact with DMSO using XPS, which

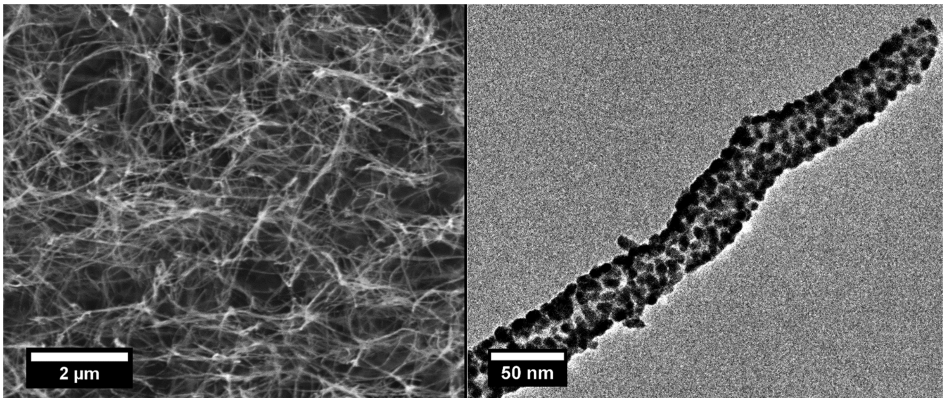

Figure 2. SEM (left) and TEM (right) images of ALD-Pt coated carbon nanotube sponge used as a cathode for extensive cycling to probe DMSO stability over long cycles (80 h round trip).

DOI: 10.1021/acsami.5b01969
ACS Appl. Mater. Interfaces 2015, 7, 11402−11411

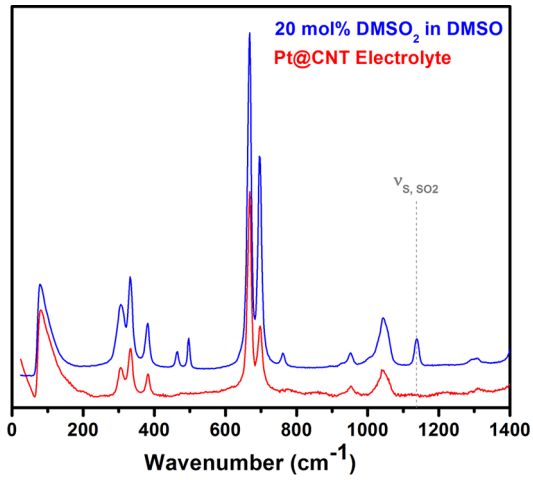

Figure 3. Raman spectrum of an electrolyte sample from Pt@CNT showing no detectable levels of $DMSO_2$ ($\nu_{S,\ SO_2}$). Shown with 20 mol % $DMSO_2$ in DMSO for comparison.

should detect solid decomposition products even from minor, self-limiting surface reactions. A previous report showed the development of carbonates at the Li_2O_2–DMSO interface after 2 days, although no reaction mechanism was suggested. We soaked commercial Li_2O_2 powder in DMSO for over 2 months inside a glovebox before removing a sample of powder, drying it under vacuum, and transferring it without atmospheric exposure to an integrated XPS (Figure S5) for analysis. Figure 4 compares the XPS signatures of the soaked powder and pristine (as received) Li_2O_2 powder transferred in the same manner. In general, the XPS results show no significant differences between the pristine and soaked powders, in support of the chemical stability of the Li_2O_2–DMSO interface. The C 1s spectrum of the pristine powder (Figure 4a) shows the presence of a hydrocarbon layer, as well as peaks associated with a small amount of lithium carbonates (290 eV) and carboxylates (288.7 eV), likely due to minor environmental exposure during manufacture or transport.[29] These features are almost completely unchanged even after more than 2 months of exposure to DMSO except for a slight increase in the carbonate peak intensity. The degree of increase in carbonate intensity is barely at the threshold of significance when fitting errors and sample-to-sample variability are considered and does not support the idea of a facile reaction between Li_2O_2 and DMSO as was previously reported. Another possibility is the reaction of Li_2O_2 with minute amounts of dissolved CO_2 in the DMSO. The O 1s spectrum of both samples (Figure 4c and 4d) are nearly identical and are consistent with Li_2O_2, with a primary peak at 531.1 eV[30] and a high binding energy tail containing contributions from various surface bound carbon–oxygen species.

XPS is unable to differentiate Li_2O_2 and LiOH due to their near-identical binding energies,[30] though subsequent XRD characterization of the soaked powder did not support the presence of LiOH or Li_2CO_3 (Figure 5). Another important element to examine for decomposition reactions is sulfur (shown in Figure 4e and 4f insets). The as-received Li_2O_2 powder was contaminated with a small amount of soluble S species (0.7 atomic percent). After 2 months, almost all of this sulfur was removed by soaking in DMSO, and no new peaks developed. In particular, we saw no evidence for the formation of $DMSO_2$, which would be expected to show a peak at approximately 169 eV.[31] Even if $DMSO_2$ was dissolved in the supporting DMSO, it would be expected to redeposit on the Li_2O_2 surface during drying. Taken together, these XPS measurements do not show any significant chemical changes which can be attributed to a decomposition reaction. DMSO from the same sample was also tested by FTIR and showed no oxidation even after 7 months, as shown in Figure 6.

Additionally, the conversion of Li_2O_2 to LiOH is expected to hinder the performance metrics of a Li–O_2 cell by halving the

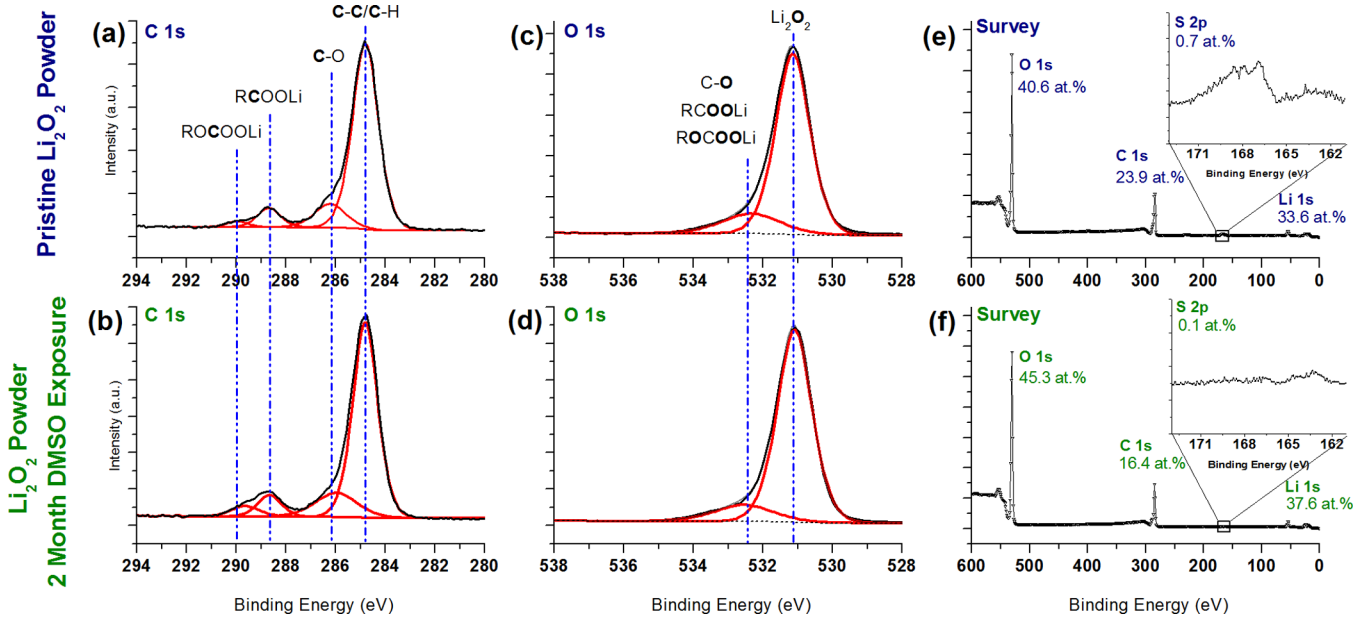

Figure 4. XPS spectra of as-received Li_2O_2 powder (a,c,e) and Li_2O_2 powder immersed in DMSO for over 2 months at room temperature (b,d,f). (a) and (b) compare the C 1s region with peak fitting, and (c) and (d) compare the O 1s region with peak fitting. (e) and (f) show a wide energy region (0–600 eV) which contains the O 1s, C 1s, S 2p, and Li 1s peaks. The numbers next to each peak reflect the calculated atomic percent composition of each sample. The insets show high resolution data from the S 2p regions. The y-scales of all graphs are normalized to approximately the same size to highlight differences in peak shape, except for the insets in (e) and (f) which have the same y-scale to highlight changes in quantity.

DOI: 10.1021/acsami.5b01969
ACS Appl. Mater. Interfaces 2015, 7, 11402–11411

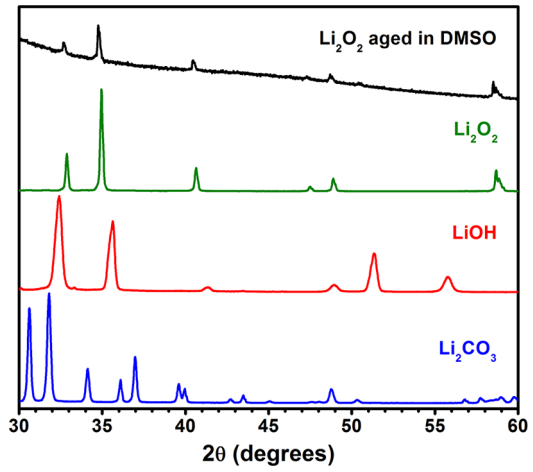

Figure 5. XRD of Li_2O_2 aged in DMSO for two months showing no indication of decomposition to LioH or Li_2CO_3.

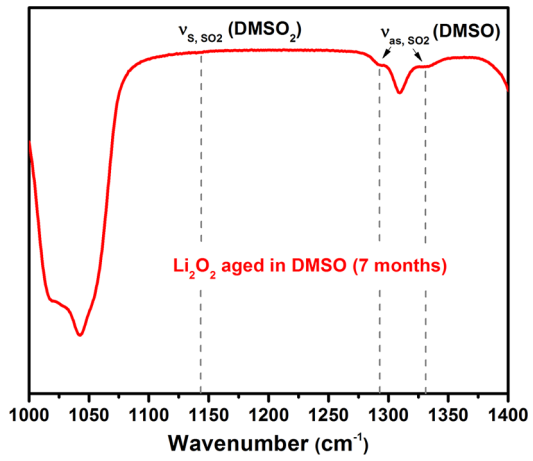

Figure 6. FTIR of Li_2O_2 aged in DMSO for seven months showing no indication of oxidation to $DMSO_2$.

capacity and requiring a charge potential significantly higher than expected for OER of Li_2O_2.[2,3,13] In an attempt to observe these effects, we closed a Li−O_2 cell with CNT cathode, discharged to a capacity of 3,000 mAh g^{-1}, and let it stand for 100 h in DMSO before charging it. If the previously proposed decomposition mechanisms[17,20] were thermodynamically favorable, a significant difference in the anodic linear scan voltammetry of the cell with and without resting time should be observed, yet the same OER capacity was recovered under 4 V, as shown in Figure S6 and further discussed in the Supporting Information. The two charging plots suggest no self-charging by chemical decomposition of the Li_2O_2 to LiOH and recovery of the same capacity by scanning anodically to 4 V. This is in good agreement with the following DFT calculations and prior experimental results, showing stability of Li_2O_2 in DMSO.

Stability of DMSO/Li_2O_2 Interface: DFT Study. In order to further support our experimental findings regarding the stability of the Li_2O_2/DMSO interface we have conducted a theoretical study of this system and report herein thermodynamic and kinetic aspects of DMSO oxidation on peroxide and superoxide-terminated surfaces of Li_2O_2.

Figure 7 depicts DMSO physisorbed on the superoxide- (left) and peroxide- (right) terminated surfaces. The $Li_{surface}$−O_{DMSO} distances are 1.95 and 2.11 Å on the peroxide-terminated surface and are larger (2.06 and 2.12 Å) on the superoxide surfaces. These bonds are shorter than Li−O bonds (2.16 Å) in bulk Li_2O_2. We consider two low-energy terminations with different oxidation states for the Li_2O_2 surface.[32] The (11−20) stoichiometric surface consists of only peroxides (O_2^{2-}) moieties, and the simulation cell has a total of 160 atoms. The other cell has oxygen rich (11−20) Li_2O_2 surfaces decorated exclusively with superoxide (O_2^-) units (144 total atoms). These low energy peroxide (O_2^{2-}) and superoxide (O_2^-) terminations of Li_2O_2 are selected to study the reactivity of different surface oxygen oxidation states toward electrolyte decomposition.

The DMSO decomposition reaction pathway studied in this work proceeds with the splitting of an O_2 dimer on the Li_2O_2 surface near the physisorbed DMSO followed by abstraction of an H atom from DMSO. The abstracted H is transferred to one of the oxygen atoms with a broken bond, forming a hydroxyl on the surface. The other oxygen atom bonds with the sulfur in DMSO, forming a $DMSO_2$−H complex. These steps appear to occur simultaneously, and no stable reaction intermediate is observed. Wannier orbital analysis[33] finds that the $DMSO_2$−H is an anion. The Li_2O_2 slab has therefore gained an H^+ and lost an oxygen atom by the end of the reaction. The energy barrier associated with decomposition determines the reaction kinetics, hence it is calculated to evaluate the probability of DMSO decomposition on Li_2O_2 by the suggested mechanism on the two different Li_2O_2 surface terminations (peroxide and superoxide).

The DFT/PBE calculations suggest that the DMSO decomposition barrier is lower on the peroxide-terminated (0.75 eV) than on the superoxide-terminated (1.43 eV) Li_2O_2 surface (Figure 8). This indicates that the decomposition is likely to occur on the peroxide-terminated surface. Also, the product of the degradation reaction is more exothermic on the peroxide (−2.08 eV) than on the superoxide-terminated (−1.20 eV) Li_2O_2 surface. We repeated this barrier calculation

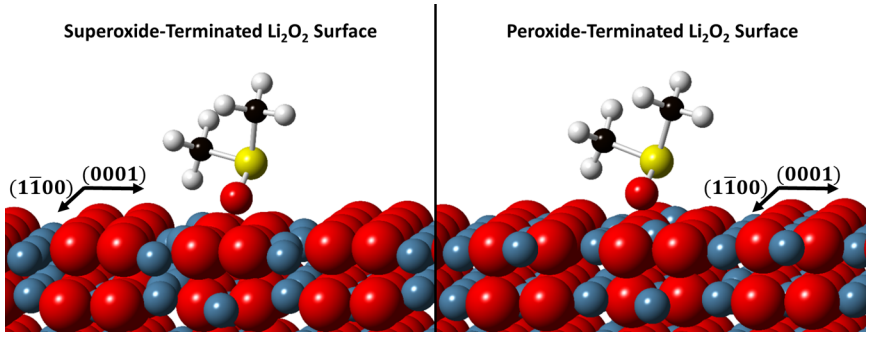

Figure 7. DMSO adsorbed atop superoxide- (left) and peroxide- (right) terminated Li_2O_2 surfaces.

DOI: 10.1021/acsami.5b01969
ACS Appl. Mater. Interfaces 2015, 7, 11402−11411

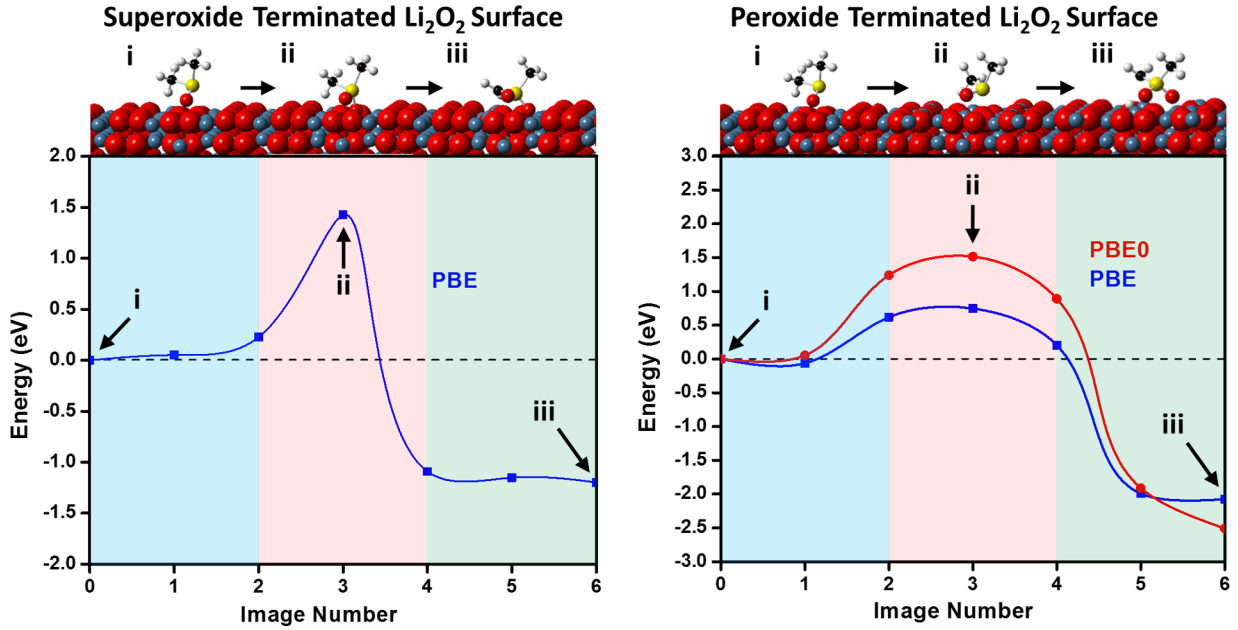

Figure 8. NEB barrier for DMSO decomposition atop superoxide- (a) and peroxide- (b) terminated Li_2O_2 surfaces. The high precision PBE0 calculation (■ (red) in (b)) predicts a higher barrier and an exothermicity that is lowered by 0.29 eV.

for the peroxide-terminated surface using a more precise, but computationally expensive, hybrid PBE0 functional. In general, hybrid functionals are known to predict more accurate (and typically larger) reaction barriers than PBE.[34] PBE0 barrier calculation results are shown in Figure 8(b). This clearly shows that the barrier for DMSO decomposition on Li_2O_2 is around double (1.42 eV) the barrier obtained from PBE (0.75 eV). Moreover, the reaction is also found to be more exothermic (−2.51 eV) than that obtained from the PBE calculation (−2.08 eV). We have estimated the reaction rate assuming Arrhenius behavior of the reactions with usual molecular vibrational prefactor of 10^{12} /s at room temperature. A reaction barrier of 1.42 eV translates into a 10^{-5} reaction/month time frame (see the SI for calculation). Hence, the PBE0 barrier suggests that the DMSO decomposition is unlikely to occur even on the peroxide-terminated surface.

Note that our PBE0-predicted DMSO reaction barrier is much higher than the DMSO (0.74 eV)[35] and TEGMDE (1.1 eV)[35] decomposition barriers on a different, high surface energy, peroxide-terminated (1−100) facet of Li_2O_2, also predicted using DFT/PBE0. Our attempt to calculate the surface energy of the facet used in ref 35 to the best of our knowledge, yielded a surface energy of (1.71 Jm^{-2}), more than 3 times higher than the surfaces considered in this work. We believe our calculations to represent the more realistic case, as lower energy surfaces are more likely to be present under the equilibrium or near-equilibrium conditions associated with battery storage or slow cycling.

Assuming that DMSO would undergo degradation following the reaction pathway studied in the present work under certain chemical/electrochemical conditions, we have conducted additional calculations to determine if the process would be self-limiting. The presumably (though unlikely) decomposed $DMSO_2$−H fragment is expected to have a strong affinity to the Li_2O_2 surface and affect subsequent decomposition reactions. Hence, we have tested the reactivity of a DMSO molecule atop a full monolayer of a broken $DMSO_2$−H covered peroxide-terminated Li_2O_2 surface. Figure 9 clearly shows that the DMSO decomposition reaction is endothermic (0.73 eV) and the barrier for the reaction is 0.76 eV when using the PBE functional. The significant unfavorable reaction suggests it does not occur to any appreciable extent. In addition, as mentioned above, the more accurate PBE0 functional should predict an even higher barrier for this reaction. This shows that even if DMSO decomposes under some chemical/electrochemical conditions, further degradation of the electrolyte is unlikely to continue via the reaction pathway presented in this work.

Finally we considered the free energy change associated with the reaction DMSO + LiO_2 → DMSO-H^-:Li^+ + HO_2 to examine the possibility of proton abstraction from DMSO by LiO_2. This calculation addresses possible formation of hydroperoxy radical/anion by O_2^- and pure DMSO, as the hydroperoxy ion was previously demonstrated to oxidize DMSO to $DMSO_2$. The reaction free energy is predicted to be +1.655 eV (+38.08 kcal mol^{-1}), an endothermic value that strongly suggests this reaction is unlikely to happen. When an explicit DMSO solvent molecule was included for LiO_2 and HO_2, the free energy change is even more endothermic, and the reaction is predicted to be even less likely to occur.

In summary, DMSO decompositions on superoxide, peroxide, and decomposed DMSO fragment-covered Li_2O_2 surfaces are predicted to either occur on time scales beyond battery life or experimental durations or are thermodynamically unfavorable.

■ DISCUSSION

The search for a suitable solvent for rechargeable Li−O_2 battery research and development is challenging, and the time frame for discovery and implementation of an optimized solvent is unclear.[9] However, fundamental and practical studies conducted in electrolytes with metastability under controlled operating conditions can provide insight regarding the desired physicochemical properties of the electrolyte and will drive progress in optimizing other components of the battery such as the cathode scaffold, separator, and anode surface.

The theoretical work presented herein, supported by the presented comprehensive experimental studies, strongly suggests that oxidation of DMSO on Li_2O_2 is very unlikely to

DOI: 10.1021/acsami.5b01969
ACS Appl. Mater. Interfaces 2015, 7, 11402−11411

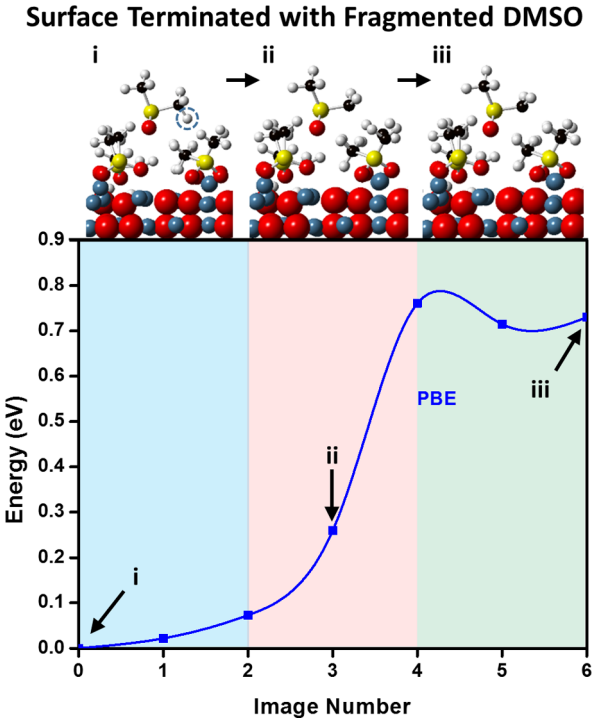

Figure 9. NEB barrier for DMSO decomposition atop a monolayer of broken DMSO on the peroxide-terminated Li_2O_2 surface. The H that is abstracted from DMSO and transferred to the broken DMSO fragment is shown with the dashed circle in Image o (Frame (i).

spontaneously occur and will take place only under certain conditions and to a minor extent when operating at the voltages between 2.65 and 4 V vs Li with an environment free of acidic groups in the electrolyte or porous scaffold.

Though recent publications raised some concerns regarding the stability of DMSO under an operating Li−O_2 battery, we believe that the results we present herein show beyond any doubts that under appropriate conditions DMSO can be used as solvent to study and to gain an important understanding of rechargeable Li−O_2 systems. We conjugate theoretical and experimental techniques to address the stability of the DMSO/Li_2O_2 interface, and we believe that this is a comprehensive approach to fully understand possible mechanisms for electrolyte decomposition in electrochemical systems.

Previously suggested mechanisms for oxidation of DMSO are presented in Scheme 1. The reaction appearing in Scheme 1a suggests conjugated oxidation of DMSO and conversion of Li_2O_2 to LiOH. However, the reaction is unbalanced with respect to both atoms and charge, making it difficult to interpret the suggested mechanism. We found no evidence for the occurrence of this reaction in our system, and the use of KO_2 as an oxidant as suggested in the relevant work was demonstrated herein to be inappropriate. Scheme 1b suggests a mechanism that involves oxidation of DMSO by O_2^- and the simultaneous reduction of O_2^- to O_2^{2-}; however, the electrochemical potential difference between O_2^- and O_2^{2-} is reported to be 1.3 V in DMSO,[21,22] and it is therefore not clear how the reaction is expected to be spontaneous.

The mechanisms presented in Scheme 1c involve the formation of a hydroperoxy radical and its reduction to hydroperoxy anion. This is with good agreement with the reaction reported by Sawyer and co-workers. However, we demonstrated herein that the source of the proton is very unlikely to be DMSO, and hence it must be abstracted from other, more

Scheme 1. Suggested Mechanisms for Oxidation of DMSO: (A),[20] (B),[18] (C),[17] and (D), the Mechanism Proposed/Studied in This Work

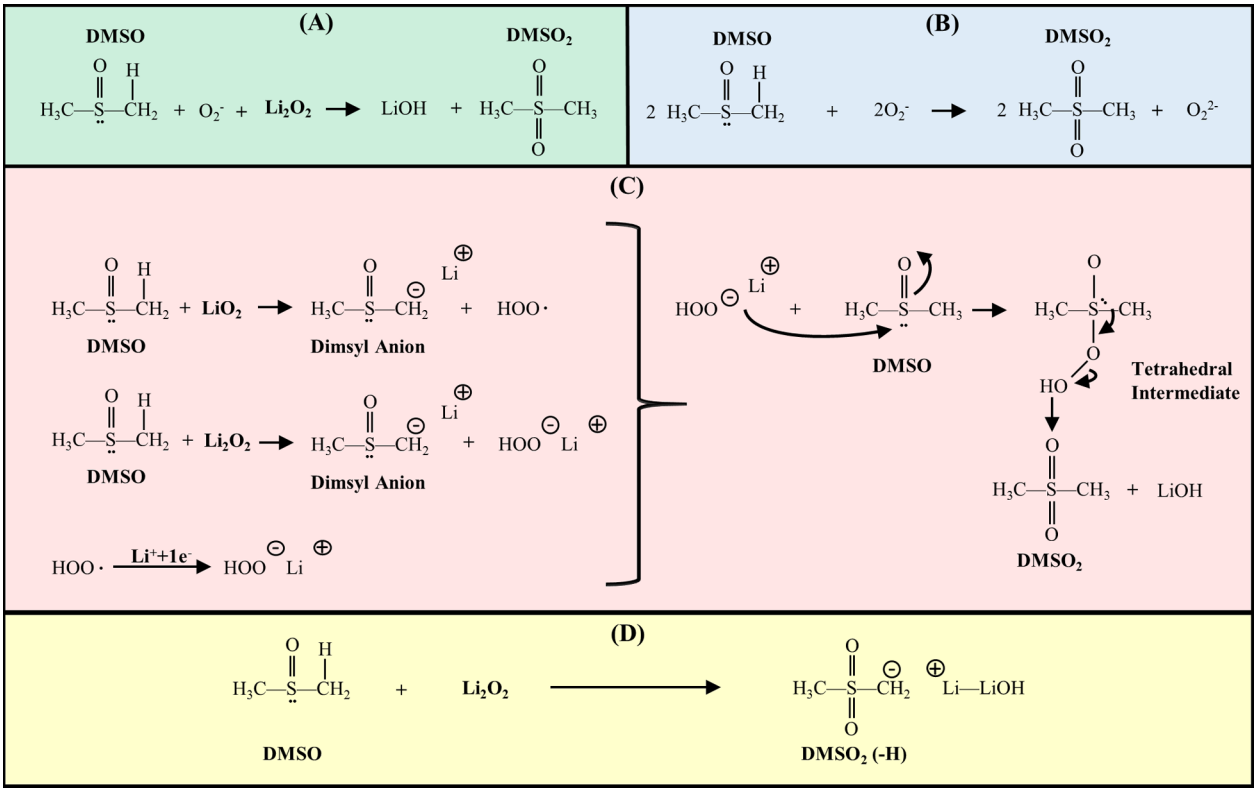

DOI: 10.1021/acsami.5b01969
ACS Appl. Mater. Interfaces 2015, 7, 11402−11411

acidic components in the system. As suggested by Sawyer and co-workers, if a source of acidic hydrogen is available in any of the cell components it may favor the oxidation of DMSO once reduced oxygen species are produced on the cathode. We suggest that the source of the proton can be in the salt,[21,22] trace H_2O,[18] or the use of activated carbon with acidic functional groups.[17,36] The pK_a of all of those components are significantly lower than the pK_a of DMSO (>31),[37] indicating that these components may be a precursor to DMSO oxidation.

Abstraction of a proton by reduced oxygen will induce the formation of a hydroperoxy anion. The strong Lewis acid (Li^+) can then coordinate with the sulfoxide oxygen of DMSO, leading to nucleophilic attack by hydroperoxy-anion on the sulfur atom of the sulfoxide and yielding a central tetrahedral intermediate as previously suggested.[17] The latter may collapse to the corresponding dimethyl sulfone ($DMSO_2$) and lithium hydroxide. Again, our work suggests that the acidity of methyl groups from DMSO itself is not strong enough to manifest proton abstraction from the DMSO molecule by Li_2O_2, suggesting that controlled exclusion of other proton sources will provide sufficiently stable conditions to prevent oxidation of DMSO on the cathode side in the potential window above 2.65 V and below the potential of anodic oxidation.

Indeed previous reports on oxidation of DMSO used water containing electrolytes,[21,23] alkyl-ammonium based electrolyte,[22] a Li−O_2 cell with self-reported leakage,[20] or microporous carbon,[17] all of which could contribute to the presence of acidic functional groups. We demonstrate that avoiding cell leakage, and hence any significant water content, together with the use of the Pt@CNT cathode in which the low concentration acidic functional groups were passivated by the ALD process, established possible conditions for a rechargeable Li−O_2 system for over 4 months of operation without noticeable oxidation of DMSO.

The operating potential is also hypothesized to affect the concentration of the superoxide and peroxide formed under ORR, with lower potentials leading to increased formation of reduced oxygen species (O_2^- or O_2^{2-} strong bases) that can abstract available weak acidic proton and facilitate the oxidation of the solvent.[18] Cell operation at potentials above 2.65 V vs Li and below 4 V in the case of the cathodes presented herein will prevent oxidation of the solvent during discharge and will enable formation of rechargeable reduced oxygen species.

Although it is not the main focus of this work and may be further addressed in following studies, the anodic stability of DMSO during charge, in the presence of O_2, is reported to be dependent on the cathode material and will take place at potentials above 4 V on amorphous microporous carbon[17] or 4.2 V in the case of Au\Pt electrodes.[17,18] In the cathodes presented herein, anodic oxidation was not obtained by Raman for a cell operated below 4 V.

The porosity of the cathode may also be of great significance, since reduced oxygen in microporous cathodes (pore <2 nm) may form a locally high concentration of O_2^- with a relatively low local concentration of DMSO.[17] Our cathodes are mesoporous, and the mobility of the solvent molecules and reduced oxygen species is not anticipated to form this kind of locally high ratio between O_2^- and DMSO.

CONCLUSIONS

We have presented theoretical and experimental evidence for the chemical and electrochemical stability of the DMSO/Li_2O_2 interface under storage and operational conditions of a Li−O_2 battery. Our theoretical models predict that DMSO decomposition on superoxide, peroxide, and decomposed DMSO fragment-covered Li_2O_2 surfaces will either occur on time scales beyond experimental durations or are thermodynamically unfavorable. Experimentally, we demonstrated no surface change of Li_2O_2 aged in DMSO and no oxidation of DMSO even after 7 months of storage. We synthesized the core−shell Pt@CNT Li−O_2 cathode via ALD and used it to further demonstrate long-term operation of a Li−O_2 rechargeable battery with DMSO as the solvent for more than 4 months of continuous cycling, with a round trip cycle length of 80 h when operated within a voltage range of 2.65−4 V vs Li/Li^+. We show that the presence of $DMSO_2$ cannot be measured effectively in the presence of $K^{16}O_2/Li^{16}O_2$ by Raman/FTIR due to the overlap between KO_2 and $DMSO_2$ in Raman and IR. Our findings strongly suggest that DMSO is a stable solvent for Li−O_2 cathode testing within a potential window of 2.65−4 V, implying that DMSO is suitable for fundamental studies of Li−O_2 cells.

EXPERIMENTAL METHODS

Materials. DMSO (Anhydrous, Sigma-Aldrich) was used without further treatment. $LiClO_4$ (Sigma-Aldrich) was thoroughly baked in a vacuum oven before making the electrolyte solution. Electrolyte was tested by Karl Fischer coulometer (899 Metrohm) before use and found to have less than 20 ppm of H_2O. Commercial high purity anhydrous Li_2O_2, LiOH, Li_2CO_3, and KO_2 (Sigma-Aldrich) were opened and stored inside the glovebox.

Characterization. High resolution imaging of the cathodes was captured with a Hitachi SU-70 scanning electron microscope (SEM) and a JEOL JEM-2100 LaB6 transmission electron microscope (TEM).

XPS analysis of aged Li_2O_2 in DMSO was measured with a Kratos AXIS Ultra DLD instrument using monochromated Al Kα X-rays as the excitation source. It is important to note that the XPS presented here was performed under rigorous air exclusion via direct transfer from an M-Braun Ar-filled glovebox to the XPS with an integrated high-vacuum transfer system, so the surface chemistry is believed to be unaltered. The instrument was operated in hybrid (magnetic immersion) mode using the slot aperture. Survey spectra were taken with a step size of 1 eV and a pass energy of 160 eV. High resolution spectra were collected using pass energy 20 eV and a 0.1 or 0.05 eV step size. Charge compensation was provided with the Kratos charge neutralization system in order to eliminate differential charging. Peak fitting was performed using CasaXPS, using 50/50 Gaussian/Lorentzian line shapes on a Shirley background. Quantification was performed using peak area corrected for the photoionization cross section of each element and the instrument geometry.

Fourier transform infrared spectroscopy was performed with a Thermo Nicolet NEXUS 670 system using an attenuated total reflectance (ATR) module. Raman spectroscopy was performed with a Horiba Jobin Yvon LabRam ARAMIS system. A 633 nm HeNe laser was used as the excitation source. The Li_2O_2 aged in DMSO was prepared/stored in a glovebox with a concentration of ∼1:25 mol Li_2O_2:DMSO.

Electrochemistry. All electrochemical measurements were performed with a Biologic VSP or Arbin BT2000 with a Li−O_2 custom cell design utilized by a few of the leading Li−O_2 research groups, as shown in Figure S2. A 5/8" diameter disc of 0.03" thick lithium foil (Alfa Aesar 99% trace metals basis) was pressed into the inset of the anode current collector, wetted with 80 μL of electrolyte, and covered with two 1" diameter Celgard 3400 polypropylene separators. The cathode (∼0.4 mg_{MWCNT})was then centered on the separators and wetted with another 80 μL of electrolyte. Finally, a stainless steel mesh current collector was placed over the MWCNT sponge, and the cell was closed. Once sealed, the cells were removed from the glovebox and purged using O_2 (Praxair 99.999%) at 15 psi (gauge) for 20 s before resealing the handvalves.

DOI: 10.1021/acsami.5b01969
ACS Appl. Mater. Interfaces 2015, 7, 11402−11411

Calculations. Electrolyte degradation studies are done using 4 × 2 surface unit cells with 5-layer thick Li_2O_2 slabs. The dimensions of these simulation cells are 10.95 × 15.38 × 24 Å. The two surfaces of the Li_2O_2 slabs, with a DMSO molecule adsorbed, are separated by at least 12 Å. The choice of (11-20) surface is motivated by the fact that this termination has either exclusively peroxide-only or superoxide-only surfaces. The more stable (0001) Li_2O_2 termination contains a mixture of peroxide and superoxide on the surface, rendering it difficult to isolate the effect of oxidation state against electrolyte stability. Moreover, the reaction barriers for the DMSO decomposition pathways obtained with the low-energy (11-20) termination, in the present study, is expected to increase when a more stable[32,38] (0001) surface is employed.

Spin-polarized DFT calculations with dipole corrections are conducted using the Vienna *ab initio* Simulation Package (VASP).[39−41] Core−valence electrons interactions are treated with a frozen-core projector-augmented wave (PAW) scheme.[42,43] The PBE exchange-correlation functional in combination with a fully self-consistent technique for treating dispersion interactions (optB88-vdW)[44−46] is used in most cases. Some of the calculations use the more accurate but computationally expensive hybrid DFT PBE0[47,48] functional containing 25% Hartree−Fock exchange, without vdW corrections. PBE0 generally gives more accurate and higher reaction barriers than PBE because the latter exhibits a substantial delocalization error which allows electrons to be unphysically delocalized on the two atoms connected by the bond being severed.[49] Whenever both PBE0 and PBE results are reported, the former is taken to be the more accurate prediction.

The wave functions of the valence electrons are expanded in a 400 eV plane wave basis set, and Γ-point k-space Brillouin zone sampling is used. The bottom three layers of the slabs are held fixed, while all other atoms are allowed to relax until the forces are less than 0.05 eV/Å in vdW-augmented PBE calculations and less than 0.08 eV/Å for the computationally expensive PBE0 calculations, respectively. Static, climbing-image nudge elastic band (NEB) calculations[50] are used to determine the reaction barriers.

It is also important to address the electrochemical conditions under which DMSO decomposition calculations are conducted. Comprehensive calculations of the voltage in simulation cells require modeling liquid DMSO-solid electrode interfaces and net surface charges, as demonstrated with graphitic surfaces.[51] This will be considered in future work. Here we confine ourselves to computing "redox potentials" associated with Li removal at the surfaces of these two Li_2O_2 slabs, which should be adequate for this redox-active cathode material. The equilibrium redox potential is defined as the difference between the energy cost of Li removal and lithium metal cohesive energy per Li atom. These calculations are conducted using the PBE functional in the absence of DMSO (see the SI).

We also consider proton abstraction from DMSO by LiO_2. The reaction involved is DMSO + LiO_2 → DMSO-H^-:Li^+ + HO_2. Here LiO_2 is Li^+ bound to superoxide with a net spin, HO_2 is H^+ bound to superoxide (with net spin), and DMSO-H^-:Li^+ is a complex obtained by removing a H^+ from DMSO and adding a Li^+ coordinated to the O atom (no net spin). All four species are charge neutral. These calculations were conducted using the g09 suite of programs, a purely dielectric continuum solvation approximation ("SMD"[52] with epsilon_o=40), the PBE0 functional, a 6-31+G(d,p) basis for geometry optimization, a 6-311++G(3df,2pd) basis for final single point energy, and harmonic approximation of thermal effects.

■ ASSOCIATED CONTENT

Supporting Information

Limit of detection for Raman/FTIR of $DMSO_2$ in DMSO, additional electrochemistry, schematics of infrastructure, and basic calculations. The Supporting Information is available free of charge on the ACS Publications website at DOI: 10.1021/acsami.5b01969.

■ AUTHOR INFORMATION

Corresponding Author

*E-mail: mnoked@gmail.com.

Author Contributions

The manuscript was written through contributions of all authors. All authors have given approval to the final version of the manuscript. M.A.S., N.K., and A.J.P. contributed equally.

Funding

This work was supported as part of the Nanostructures for Electrical Energy Storage (NEES), an Energy Frontier Research Center (EFRC) funded by the U.S. Department of Energy, Office of Science, Basic Energy Sciences under Award number DESC0001160. Contributions by N.K. were made while at Sandia National Laboratories under EFRC sponsorship. M. A. Schroeder acknowledges a graduate fellowship through the John and Maureen Hendricks Charitable Foundation. M. Noked acknowledges a postdoctoral fellowship through the Fulbright Program.

Notes

The authors declare no competing financial interest.

■ ACKNOWLEDGMENTS

We acknowledge the support of the Maryland Nanocenter and its NispLab.

■ REFERENCES

(1) Bruce, P. G.; Freunberger, S. A.; Hardwick, L. J.; Tarascon, J.-M. Li−O_2 and Li−S Batteries with High Energy Storage. *Nat. Mater.* **2012**, *11*, 19−29.

(2) Girishkumar, G.; McCloskey, B.; Luntz, A. C.; Swanson, S.; Wilcke, W. Lithium-Air Battery: Promise and Challenges. *J. Phys. Chem. Lett.* **2010**, *1*, 2193−2203.

(3) Kraytsberg, A.; Ein-Eli, Y. Review on Li-Air Batteries - Opportunities, Limitations and Perspective. *J. Power Sources* **2011**, *196*, 886−893.

(4) Christensen, J.; Albertus, P.; Sanchez-Carrera, R. S.; Lohmann, T.; Kozinsky, B.; Liedtke, R.; Ahmed, J.; Kojic, A. A Critical Review of Li/Air Batteries. *J. Electrochem. Soc.* **2012**, *159*, R1.

(5) Wang, Z.-L.; Xu, D.; Xu, J.-J.; Zhang, X.-B. Oxygen Electrocatalysts in Metal-Air Batteries: From Aqueous to Nonaqueous Electrolytes. *Chem. Soc. Rev.* **2013**, DOI: 10.1039/c3cs60248f.

(6) Capsoni, D.; Bini, M.; Ferrari, S.; Quartarone, E.; Mustarelli, P. Recent Advances in the Development of Li-Air Batteries. *J. Power Sources* **2012**, *220*, 253−263.

(7) Bryantsev, V. S.; Giordani, V.; Walker, W.; Blanco, M.; Zecevic, S.; Sasaki, K.; Uddin, J.; Addison, D.; Chase, G. V. Predicting Solvent Stability in Aprotic Electrolyte Li-Air Batteries: Nucleophilic Substitution by the Superoxide Anion Radical ($O_2^{\bullet-}$). *J. Phys. Chem. A* **2011**, *115*, 12399−12409.

(8) Freunberger, S. A.; Chen, Y.; Drewett, N. E.; Hardwick, L. J.; Bardé, F.; Bruce, P. G. The Lithium-Oxygen Battery with Ether-Based Electrolytes. *Angew. Chem., Int. Ed.* **2011**, *50*, 8609−8613.

(9) Johnson, L.; Li, C.; Liu, Z.; Chen, Y.; Freunberger, S. A.; Ashok, P. C.; Praveen, B. B.; Dholakia, K.; Tarascon, J.-M.; Bruce, P. G. The Role of LiO_2 Solubility in O_2 Reduction in Aprotic Solvents and Its Consequences for Li−O_2 Batteries. *Nat. Chem.* **2014**, *6*, 1091−1099.

(10) Laoire, C. O.; Mukerjee, S.; Abraham, K. M.; Plichta, E. J.; Hendrickson, M. A. Influence of Nonaqueous Solvents on the Electrochemistry of Oxygen in the Rechargeable Lithium-Air Battery. *J. Phys. Chem. C* **2010**, *114*, 9178−9186.

(11) Peng, Z.; Freunberger, S. A.; Hardwick, L. J.; Chen, Y.; Giordani, V.; Bardé, F.; Novák, P.; Graham, D.; Tarascon, J. M.; Bruce, P. G. Oxygen Reactions in a Non-Aqueous Li+ Electrolyte. *Angew. Chem., Int. Ed.* **2011**, *50*, 6351−6355.

DOI: 10.1021/acsami.5b01969
ACS Appl. Mater. Interfaces 2015, 7, 11402−11411

(12) Sharon, D.; Etacheri, V.; Garsuch, A.; Afri, M.; Frimer, A. A.; Aurbach, D. On the Challenge of Electrolyte Solutions for Li-Air Batteries: Monitoring Oxygen Reduction and Related Reactions in Polyether Solutions by Spectroscopy and EQCM. *J. Phys. Chem. Lett.* **2013**, *4*, 127−131.
(13) Luntz, A. C.; Mccloskey, B. D. Nonaqueous Li-Air Batteries: A Status Report. *Chem. Rev.* **2014**, *114*, 11721−11750.
(14) Lu, Y.-C.; Gallant, B. M.; Kwabi, D. G.; Harding, J. R.; Mitchell, R. R.; Whittingham, M. S.; Shao-Horn, Y. Lithium-Oxygen Batteries: Bridging Mechanistic Understanding and Battery Performance. *Energy Environ. Sci.* **2013**, *6*, 750−768.
(15) Schwenke, K. U.; Meini, S.; Wu, X.; Gasteiger, H. A.; Piana, M. Stability of Superoxide Radicals in Glyme Solvents for Non-Aqueous Li-O_2 Battery Electrolytes. *Phys. Chem. Chem. Phys.* **2013**, *15*, 11830−11839.
(16) Ottakam Thotiyl, M. M.; Freunberger, S. A.; Peng, Z.; Chen, Y.; Liu, Z.; Bruce, P. G. A Stable Cathode for the Aprotic Li-O_2 Battery. *Nat. Mater.* **2013**, *12*, 1050−1056.
(17) Sharon, D.; Afri, M.; Noked, M.; Garsuch, A.; Frimer, A. A.; Aurbach, D. Oxidation of Dimethly Sulfoxide Solutions by Electrochemical Reduction of Oxygen. *J. Phys. Chem. Lett.* **2013**, *4*, 3115−3119.
(18) Mozhzhukhina, N.; Méndez De Leo, L. P.; Calvo, E. J. Infrared Spectroscopy Studies on Stability of Dimethyl Sulfoxide for Application in a Li-Air Battery. *J. Phys. Chem. C* **2013**, *117*, 18375−18380.
(19) Younesi, R.; Norby, P.; Vegge, T. A New Look at the Stability of Dimethyl Sulfoxide and Acetonitrile in Li-O_2 Batteries. *ECS Electrochem. Lett.* **2014**, *3*, A15−A18.
(20) Kwabi, D. G.; Batcho, T. P.; Amanchukwu, C. V.; Ortiz-Vitoriano, N.; Hammond, P.; Thompson, C. V.; Shao-Horn, Y. Chemical Instability of Dimethyl Sulfoxide in Lithium−Air Batteries. *J. Phys. Chem. Lett.* **2014**, *5*, 2850−2856.
(21) Goolsby, A. D.; Sawyer, D. T. The Electrochemical Reduction of Superoxide Ion and Oxidation of Hydroxide Ion in Dimethyl Sulfoxide. *Anal. Chem.* **1968**, *40*, 83−86.
(22) Merritt, M. V.; Sawyer, D. T. Electrochemical Studies of the Reactivity of Superoxide Ion with Several Alkyl Halides in Dimethyl Sulfoxide. *J. Org. Chem.* **1970**, *35*, 2157−2159.
(23) Krtil, P.; Kavan, L.; Hoskovcová, I.; Kratochvilová, K. Anodic Oxidation of Dimethyl Sulfoxide Based Electrolyte Solutions: Anin Situ FTIR Study. *J. Appl. Electrochem.* **1996**, *26*, 523−527.
(24) Gittleson, F. S.; Ryu, W.-H.; Taylor, A. D. Operando Observation of the Gold−Electrolyte Interface in Li−O_2 Batteries. *ACS Appl. Mater. Interfaces* **2014**, *6*, 19017−19025.
(25) Duerr, K.; Olah, J.; Davydov, R.; Kleimann, M.; Li, J.; Lang, N.; Puchta, R.; Hübner, E.; Drewello, T.; Harvey, J. N.; Norbert, J.; Ivanović-Burmazović, I. Studies on an Iron(iii)-Peroxo Porphyrin. Iron(III)-Peroxo or iron(II)-Superoxo? *Dalton Trans.* **2010**, *39*, 2049−2056.
(26) Ottakam Thotiyl, M. M.; Freunberger, S. A.; Peng, Z.; Bruce, P. G. The Carbon Electrode in Nonaqueous Li-O_2 Cells. *J. Am. Chem. Soc.* **2013**, *135*, 494−500.
(27) Peng, Z.; Freunberger, S. A.; Chen, Y.; Bruce, P. G. A Reversible and Higher-Rate Li-O_2 Battery. *Science (80-.)* **2012**, *337*, 563−566.
(28) Legrand, L.; Tranchant, A.; Messina, R.; Romain, F.; Lautie, A. Raman Study of Aluminum Chloride-Dimethylsulfone Solutions. *Inorg. Chem.* **1996**, *35*, 1310−1312.
(29) Herstedt, M.; Abraham, D. P.; Kerr, J. B.; Edström, K. X-Ray Photoelectron Spectroscopy of Negative Electrodes from High-Power Lithium-Ion Cells Showing Various Levels of Power Fade. *Electrochim. Acta* **2004**, *49*, 5097−5110.
(30) Yao, K. P. C.; Kwabi, D. G.; Quinlan, R. A.; Mansour, A. N.; Grimaud, A.; Lee, Y.-L.; Lu, Y.-C.; Shao-Horn, Y. Thermal Stability of Li_2O_2 and Li_2O for Li-Air Batteries: In Situ XRD and XPS Studies. *J. Electrochem. Soc.* **2013**, *160*, A824−A831.
(31) Lindberg, B. J.; Hamrin, K.; Johansson, G.; Gelius, U.; Fahlman, A.; Nordling, C.; Siegbahn, K. Molecular Spectroscopy by Means of ESCA II. Sulfur Compounds. Correlation of Electron Binding Energy with Structure. *Phys. Scr.* **1970**, *1*, 286−298.
(32) Radin, M. D.; Rodriguez, J. F.; Tian, F.; Siegel, D. J. Lithium Peroxide Surfaces Are Metallic, While Lithium Oxide Surfaces Are Not. *J. Am. Chem. Soc.* **2012**, *134*, 1093−1103.
(33) Marzari, N.; Vanderbilt, D. Maximally-Localized Generalized Wannier Functions for Composite Energy Bands. *Phys. Rev. B* **1997**, *56*, 22.
(34) Sai, N.; Leung, K.; Zádor, J.; Henkelman, G. First Principles Study of Photo-Oxidation Degradation Mechanisms in P3HT for Organic Solar Cells. *Phys. Chem. Chem. Phys.* **2014**, *16*, 8092−8099.
(35) Laino, T.; Curioni, A. Chemical Reactivity of Aprotic Electrolytes on a Solid Li_2O_2 Surface: Screening Solvents for Li-Air Batteries. *New J. Phys.* **2013**, *15*, 095009.
(36) Ania, C. O.; Khomenko, V.; Raymundo-Piñero, E.; Parra, J. B.; Béguin, F. The Large Electrochemical Capacitance of Microporous Doped Carbon Obtained by Using a Zeolite Template. *Adv. Funct. Mater.* **2007**, *17*, 1828−1836.
(37) Matthews, W. S.; Bares, J. E.; Bartmess, J. E.; Bordwell, F. G.; Cornforth, F. J.; Drucker, G. E.; Margolin, Z.; McCallum, R. J.; McCollum, G. J.; Vanier, N. R. Equilibrium Acidities of Carbon Acids. VI. Establishment of an Absolute Scale of Acidities in Dimethyl Sulfoxide Solution. *J. Am. Chem. Soc.* **1975**, *97*, 7006−7014.
(38) Radin, M. D.; Tian, F.; Siegel, D. J. Electronic Structure of Li_2O_2 {0001} Surfaces. *J. Mater. Sci.* **2012**, *47*, 7564−7570.
(39) Kresse, G. Efficient Iterative Schemes for Ab Initio Total-Energy Calculations Using a Plane-Wave Basis Set. *Phys. Rev. B* **1996**, *54*, 11169−11186.
(40) Kresse, G.; Furthmüller, J. Efficiency of Ab-Initio Total Energy Calculations for Metals and Semiconductors Using a Plane-Wave Basis Set. *Comput. Mater. Sci.* **1996**, *6*, 15−50.
(41) Paier, J.; Marsman, M.; Kresse, G. Why Does the B3LYP Hybrid Functional Fail for Metals? *J. Chem. Phys.* **2007**, *127*, 024103.
(42) Kresse, G. From Ultrasoft Pseudopotentials to the Projector Augmented-Wave Method. *Phys. Rev. B* **1999**, *59*, 1758−1775.
(43) Blöchl, P. E. Projector Augmented-Wave Method. *Phys. Rev. B* **1994**, *50*, 17953−17979.
(44) Klimeš, J.; Bowler, D. R.; Michaelides, A. Chemical Accuracy for the van Der Waals Density Functional. *J. Phys.: Condens. Matter* **2010**, *22*, 022201.
(45) Klimeš, J.; Bowler, D. R.; Michaelides, A. Van Der Waals Density Functionals Applied to Solids. *Phys. Rev. B: Condens. Matter Mater. Phys.* **2011**, *83*, 195131.
(46) Dion, M.; Rydberg, H.; Schröder, E.; Langreth, D. C.; Lundqvist, B. I. Van Der Waals Density Functional for General Geometries. *Phys. Rev. Lett.* **2004**, *92*, 246401−1.
(47) Perdew, J. P.; Ernzerhof, M.; Burke, K. Rationale for Mixing Exact Exchange with Density Functional Approximations. *J. Chem. Phys.* **1996**, *105*, 9982.
(48) Adamo, C.; Barone, V. Toward Reliable Density Functional Methods without Adjustable Parameters: The PBE0Model. *J. Chem. Phys.* **1999**, *110*, 6158.
(49) Mori-Sánchez, P.; Cohen, A. J.; Yang, W. Localization and Delocalization Errors in Density Functional Theory and Implications for Band-Gap Prediction. *Phys. Rev. Lett.* **2008**, *100*, 146401.
(50) Henkelman, G.; Jónsson, H. Improved Tangent Estimate in the Nudged Elastic Band Method for Finding Minimum Energy Paths and Saddle Points. *J. Chem. Phys.* **2000**, *113*, 9978−9985.
(51) Leung, K. Predicting the Voltage Dependence of Interfacial Electrochemical Processes at Lithium-Intercalated Graphite Edge Planes. *Phys. Chem. Chem. Phys.* **2015**, *17*, 1637−1643.
(52) Marenich, A. V.; Cramer, C. J.; Truhlar, D. G. Universal Solvation Model Based on Solute Electron Density and on a Continuum Model of the Solvent Defined by the Bulk Dielectric Constant and Atomic Surface Tensions. *J. Phys. Chem. B* **2009**, *113*, 6378−6396.

DOI: 10.1021/acsami.5b01969
ACS Appl. Mater. Interfaces 2015, 7, 11402−11411